Report no. changed (Mar 2006): SM-348-UU

SACLANTCEN MEMORANDUM
serial no.: SM-348

SACLANT UNDERSEA RESEARCH CENTRE MEMORANDUM

MODELLING OF SCATTERING BY PARTIALLY BURIED ELASTIC CYLINDERS

J.A. Fawcett

February 1998

Report no. changed (Mar 2006): SM-348-UU

SACLANT Undersea Research Centre
Viale San Bartolomeo 400
19138 San Bartolomeo (SP), Italy

tel: +39-187-540.111
fax: +39-187-524.600

e-mail: library@saclantc.nato.int

NORTH ATLANTIC TREATY ORGANIZATION

SACLANTCEN SM-348

Modelling of scattering by partially buried elastic cylinders

John A. Fawcett

The content of this document pertains to work performed under Project 033-3 of the SACLANTCEN Programme of Work. The document has been approved for release by The Director, SACLANTCEN.

Jan L. Spoelstra
Director

intentionally blank page

Modelling of scattering by partially buried elastic cylinders

John A. Fawcett

Executive Summary: The ability to model the acoustic scattering characteristics of bottom laid objects is an important issue for sonar system design and performance prediction. Under certain environmental conditions, bottom laid objects can also become partially or completely buried into ocean sediments. For proud and partially buried targets, target scattering consists of interfering contributions due to direct path energy (source to target to receiver), and energy that has interacted with the sediment either before or after interacting with the target. These interactions with the sediment can enhance or lessen the overall backscattering from the target (compared to the free-space characteristics) depending on the constructive or destructive nature of the interference. For completely buried targets, all energy scattered from the target must first be transmitted into the sediment. This transmitted energy also plays a role in the scattering characteristics for partially buried targets. For some types of sediment (including most sandy seabeds), low grazing angle source geometries result in transmitted energy levels in the sediment that fall off strongly with increasing depth into the sediment and increasing acoustic frequency. All of these effects must be taken into account in order to accurately model target scattering levels.

Previous work in this area involved development of a mathematical treatment and computer model for the case of partially or completely buried fluid cylinders. In this memorandum we outline extensions to this work so that solid or shelled cylinders can also be considered. These modifications allow for the modelling of structures with realistic spectral characteristics. The results of computations with this method are then presented both in the frequency and temporal domains as the percentage of burial of the cylinder is varied. It is hoped that in the future, models for the scattering from more realistic shapes than the idealized two-dimensional cylinder dealt with here can be developed for the case when these objects become partially or completely buried.

intentionally blank page

SACLANTCEN SM-348

Modelling of scattering by partially buried elastic cylinders

John A. Fawcett

Abstract: The work of a previous memorandum on the modelling of scattering by a partially buried cylinder is extended to allow the cylinder to have full elasticity (and not just be a fluid structure as in the previous work). The results of computations showing the effects of increasing burial on the backscattered field, both in the spectral and temporal domains, are given. A shelled and a solid aluminum cylinder are considered for a grazing angle of incidence which is subcritical.

Keywords: cylinder, partially buried

Contents

1

Introduction

The effect of burial in the seabed on the spectrum of the energy backscattered from an elastic object is an area of current research [1]-[3]. In an earlier memorandum [1] we presented a Boundary Integral Equation Method (BIEM) which could be used to model the scattering from proud (above the seabed), partially buried, or fully buried cylindrical structures. In that work the cylinder was taken to be a fluid structure; shear properties were not modelled. In this memorandum we describe a simple modification to allow the cylinder to be elastic in nature, and we present computational examples of the effect of burial on the energy (both in the spectral and temporal domains) backscattered from an evacuated steel-shelled cylinder and from a solid aluminum cylinder as they are increasingly buried in a sediment layer.

2

Theory

In this memorandum we will consider an infinitely long cylinder and use two-dimensional modelling. Of course, in the real world a cylinder has finite length. It is possible to use the two-dimensional solution and approximately account for its finite length [4-6], yielding results which are accurate for broadside geometries. In fact, if the receiver is located close to the cylinder in terms of Fresnel zone lengths then the infinite cylinder solution is a good approximation to the finite cylinder solution for broadside geometries. We expect that the above statements are also true in the case that the cylinder is partially or fully buried. Thus, although the two-dimensional theory of this memorandum has limitations in terms of modelling realistic cylinders, it could be used to yield good approximations to the three-dimensional problem.

In [1] the pressure field within the cylinder was taken to have the form

$$p = \sum_{m=-N}^{N} a_m e^{im\theta} \tag{1}$$

$$p_r = \sum_{m=-N}^{N} \alpha_m a_m e^{im\theta} \tag{2}$$

where p_r is the radial derivative of the pressure (the range being measured from the centre of the cylinder). The form of the coefficients α_m can be determined from the form of the solution in the interior of the cylinder. For example, in the case that the cylinder was a homogeneous fluid then

$$\alpha_m = \frac{1}{J_m(k_{int}r)} \frac{dJ_m(k_{int}r)}{dr}, \tag{3}$$

where the subscript "int" refers to the interior of the cylinder. In the case that the interior is a layered fluid then the interior continuity equations can be used to derive an expression for α_m. We now indicate the approach we take if the cylinder is a shelled elastic cylinder with some interior fill (a solid cylinder is a subcase of this). The outer radius of the cylinder is $r = a$ and the interior radius is $r = b$.

In the exterior fluid, at a particular angular order m, there is a single unknown compressional coefficient h_p^{ex} for the Hankel function of order m, $H_m^1(kr)$. In the shell there are 4 unknowns h_p^{es}, j_p^{es}, h_s^{es}, and j_s^{es} ("es" denotes elastic shell) where these

are the coefficients for the Hankel and Bessel functions for the compressional and shear potentials, respectively. Finally, within the innermost section of the cylinder we have j_p^{int} and j_s^{int}. Thus for a specified incident field, there is a 7×7 system of equations for the unknown coefficients $\vec{\gamma}$,

$$A\vec{\gamma} = \vec{r} \tag{4}$$

where

$$\vec{\gamma} \equiv (h_p^{ex}, j_p^{es}, h_p^{es}, j_s^{es}, h_s^{es}, j_p^{int}, j_s^{int})^T \tag{5}$$

and $\vec{r}$ has the form

$$(r_1, r_2, 0, 0, 0, 0, 0)^T, \tag{6}$$

where r_1 and r_2 are expressions involving the incident compressional potential. Thus, only the first two equations of Eq.(4) involve h_p^{ex}.

If we consider the bottom righthand 5×6 submatrix of A (i.e., the last five rows and 6 columns), A_b, and the last 6 coefficients of γ, we can write

$$A_b\gamma_b = \vec{0}. \tag{7}$$

Arbitrarily setting j_p^{es} equal to unity we can write

$$\hat{A}_b\hat{\gamma}_b = -\vec{a}_1 \tag{8}$$

where $\hat{A}_b$ is the right 5×5 submatrix of A_b, $\hat{\gamma}_b$ are the 5 unknown interior coefficients (assuming that $j_p^{es} = 1$) and $\vec{a}_1$ is the first column of A_b. Thus we can express the radial stress,σ_{rr}, and the radial displacement, u_r, at the interior surface of the cylinder in terms of the unknown coefficient for j_p^{es}. In particular,

$$\begin{aligned} \sigma_{rr} &\propto (f_1 + \hat{\gamma}_{b,1}f_2 + \hat{\gamma}_{b,2}f_3 + \hat{\gamma}_{b,3}f_4) \\ u_r &\propto (g_1 + \hat{\gamma}_{b,1}g_2 + \hat{\gamma}_{b,2}g_3 + \hat{\gamma}_{b,3}g_4) \end{aligned} \tag{9}$$

where

$$\begin{aligned} f_1 &= \frac{-\lambda\omega^2}{c_p^2}J_m + 2\mu J_m''(k_p a) \\ f_2 &= \frac{-\lambda\omega^2}{c_p^2}H_m + 2\mu H_m''(k_p a) \\ f_3 &= 2\mu i\frac{m}{a}(J_m'(k_s a) - \frac{1}{a}J_m(k_s a)) \\ f_4 &= 2\mu i\frac{m}{a}(H_m'(k_s a) - \frac{1}{a}H_m(k_s a)) \\ g_1 &= J_m'(k_p a) \\ g_2 &= H_m'(k_p a) \\ g_3 &= \frac{im}{a}J_m(k_s a) \\ g_4 &= \frac{im}{a}H_m(k_s a). \end{aligned} \tag{10}$$

The prime symbol denotes a derivative with respect to r and $\gamma_{b,i}$ denotes the ith element of the solution vector γ_b. We note that σ_{rr} and u_r are continuous across the cylinder surface and that in the surrounding fluids $p = -\sigma_{rr}$ and $p_r = -\rho\omega^2 u_r$. Thus we can write for the pressure p and its normal derivative p_r on the exterior of the cylinder's surface,

$$\begin{aligned} p &= \sum_{m=-N}^{N} -a_m t_m e^{im\theta} \\ p_r &= \sum_{m=-N}^{N} -\rho\omega^2 a_m u_m e^{im\theta} \end{aligned} \tag{11}$$

where t_k and u_k are the expressions in brackets in Eq.(9). The remainder of the BIEM approach follows that of [1] for the fluid cylinder. The basic BIEM now takes the form

$$2\pi a_m = i_m - A_{mk} t_k a_k + B_{mk}\omega^2 u_k a_k \tag{12}$$

where

$$A_{mk} \equiv a \lim_{\epsilon \to 0} \int_0^{2\pi} \int_0^{2\pi} G_{r'}(a+\epsilon, \theta; a, \theta') e^{-im\theta} e^{ik\theta'} d\theta d\theta' \tag{13}$$

$$B_{mk} \equiv a \lim_{\epsilon \to 0} \int_0^{2\pi} \int_0^{2\pi} G(a+\epsilon, \theta; a, \theta') e^{-im\theta} e^{ik\theta'} \rho(\theta) d\theta d\theta' \tag{14}$$

where G is the half-space Green's function. The details of computing these integrals are given in [1].

There is a problem with this approach (and also in [1]) in the case that the cylinder is partially buried. Because the fluid approximation is used for the surrounding environment, the tangential component of displacement is not continuous across the water-basement interface. Thus the displacement in the radial direction (defined with respect to the cylinder centre) is also not continuous. Hence where the cylinder's surface intersects the interface (we denote the corresponding angles as $\pm\theta_c$) we expect the series expansion of and u_r and p_r (Eq.(11)) to behave poorly. This problem is improved by the fact that the series are involved in integrals, Eqs.(13) and (14). However, for cases where the values of p_r near θ_c are particularly important in the total scattering solution, there may be poor convergence with respect to the series expansion. One ad hoc solution to this problem is to compute the numerical solution for N Fourier coefficients and then for a larger number (say N+10) (by saving the integral results for the N case, the increased computation is not large) and see if the solutions are sufficiently converged. If they are not, this computed value should be ignored or replaced by a smoothed value.

3

Numerical examples

3.1 Steel-shelled cylinder with an evacuated interior

As a numerical example, we first consider a steel-shelled cylinder (6 mm thick) with an evacuated interior (which we model by using near zero values of c_p,c_s and ρ) and an outer radius of 0.25 m. We consider the water with sound speed 1500 m/s and ρ = 1 g/cm^3 overlying the basement with sound speed 1700 m/s and ρ=1.5 g/cm^3. The steel has parameters: c_p = 5950 m/s, c_s = 3240 m/s and ρ= 7.7 g/cm^3. We consider an incident plane-wave, comprised of the direct and reflected wave in the water column and the transmitted wave in the basement (see Fig. 1). The grazing angle of incidence is 18.4° which is significantly subcritical. A receiver is in the water column at a range of 3.16 m at an angle of 18.4° with respect to the origin on the interface. In Figs. 2a-2c we present the spectra of the backscattered energy

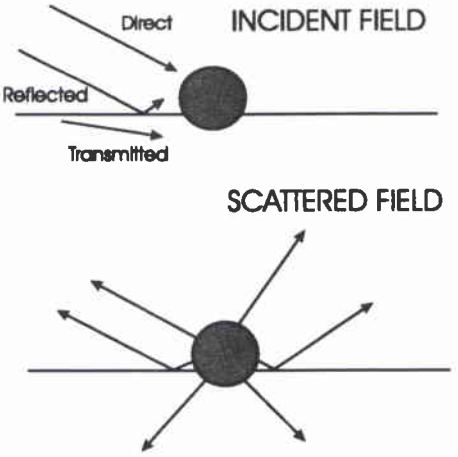

Figure 1: *Schematic of geometry for partially-buried cylinder with direct and reflected planes waves incident in the water column and evanescent wave in the bottom*

for 15 levels of fractional burial of the cylinder, starting at a burial of -1.5a and ending with a burial depth of 1.3a. Fractional burial depth denotes the number of cylinder radii that the cylinder is offset from the interface. In terms of percentages, an offset of 1 radius above the interface is 0% burial and an offset of 1 radius below the interface corresponds to 100% burial.

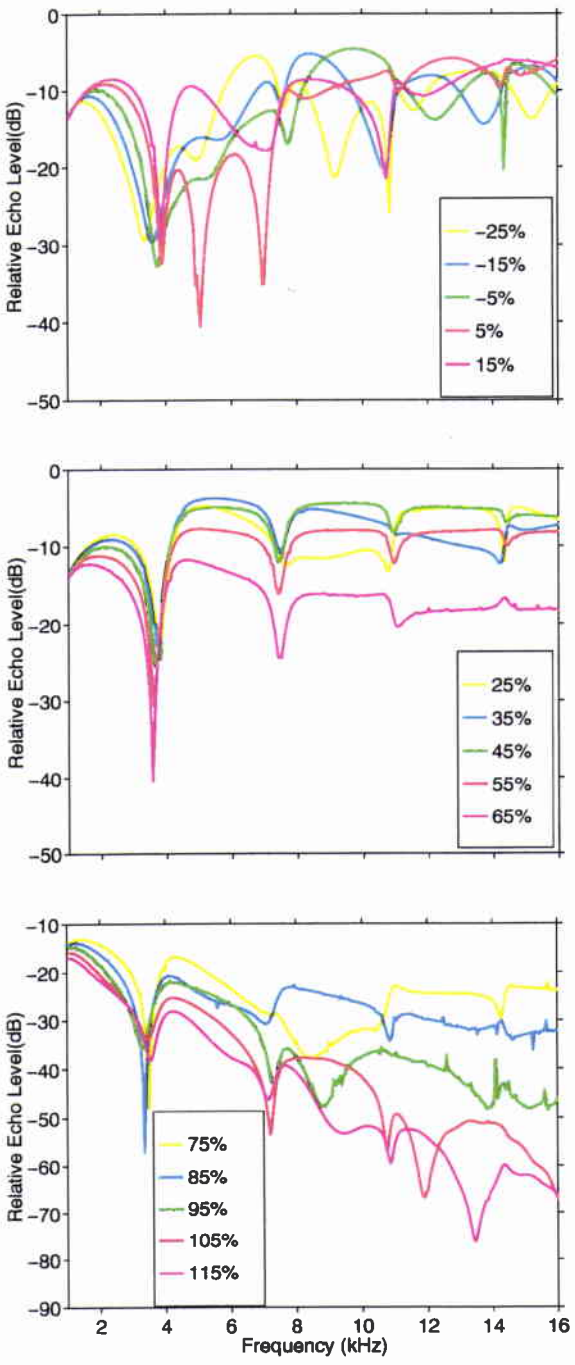

Figure 2: *Plots of backscattered power spectra from steel-shelled cylinder as a function of fractional burial, from above the seabed interface to totally buried.*

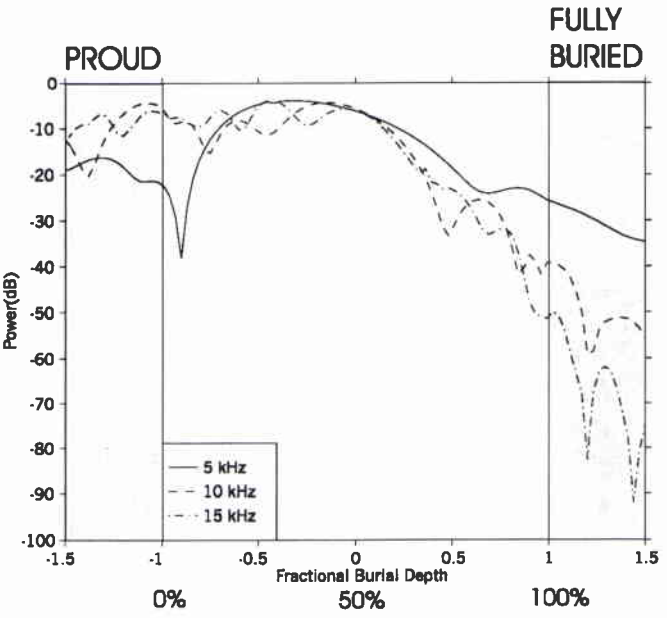

Figure 3: *Backscattered power levels from steel-shelled cylinder as a function of fractional burial for 5, 10, and 15 kHz.*

In Fig. 2a the cylinder is either proud or slightly buried; in these cases the interference effects between the direct and seabed-reflected energy are evident. For the curves of Fig. 2b the cylinder has become significantly buried and although there is a decrease in amplitude with increasing burial, the curves look similar to each other. For these curves, the direct and reflected raypaths for the source/receiver/object are almost identical to each other and hence the interference effects are less. Finally, in Fig. 2c the cylinder is totally or almost totally buried. There is a rapid decrease in backscattering amplitude for increasing frequency (for burials $\geq 95\%$) and the last 2 curves are starting to show some interference effects. Also the 85% and 95% curves seem to show some numerical problems at some of the higher frequencies (although, it is difficult to know sometimes whether a particular frequency corresponds to a resonance or the spectral amplitude is numerically inaccurate).

We now give a different presentation of the spectral information. We consider the frequency fixed at 5, 10, and 15 kHz and in Fig. 3 show the variation of the backscattered level with respect to the fraction of burial. We have computed these curves for 101 depths of burial. As can be seen for fractions of burial, slightly less than 0 (50% burial), the fall-off of amplitude is rapid, more rapid with increasing frequency, as one would expect due to the evanescent nature of the energy in the bottom.

Thus far we have dealt with the amplitude or power of the backscattered spectra. However, the phase of the spectra is also important when Fourier synthesizing the time domain scattered pulse. We construct the scattered pulse in the time domain

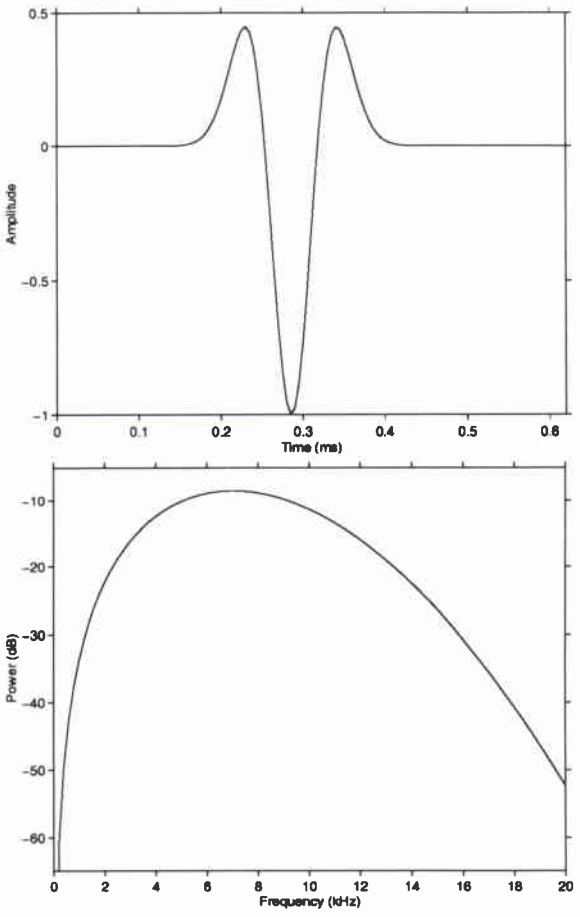

Figure 4: *Ricker pulse used in time domain computations and the corresponding power spectrum*

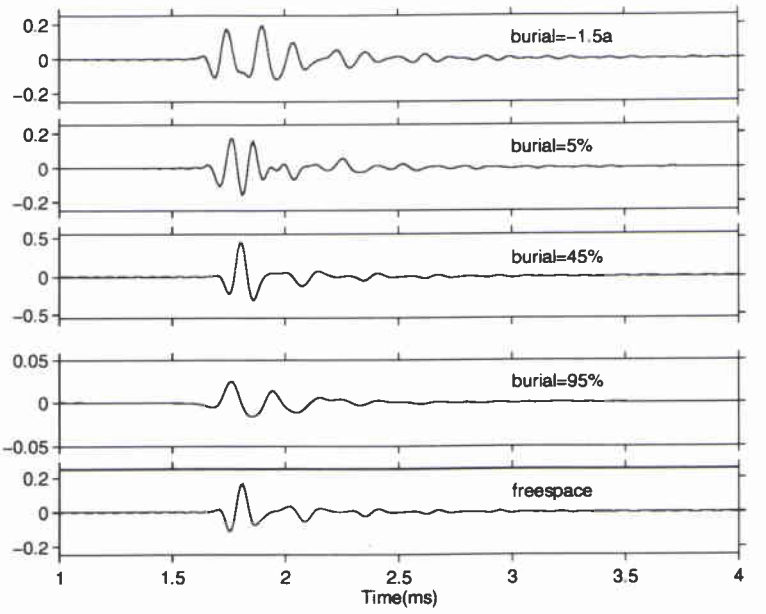

Figure 5: *Backscattered time series from steel-shelled cylinder as a function of fractional burial. (Please note the scale change in plots 3 and 4.)*

by multiplying the complex-valued Fourier spectra with the source spectrum for a 7-kHz Ricker wavelet; the Ricker wavelet in the time domain and its spectrum are shown in Fig. 4.

The resulting time series are shown in Fig. 5 for different amounts of fractional burial: $1.5a$ above the interface, burial of 5%, burial of 45%, and burial of 95%. Also shown is the time series for the cylinder surrounded only by water. For the first two curves there is coherent combination of the direct and reflected wavefields for both the incident and scattered wavefields. This has the effect of producing a sequence of overlapping pulses for the top time series. These pulses become increasingly merged in time until for values of burial near 50%, the resultant pulse is similar to that scattered by the cylinder in freespace but there is an amplitude enhancement by a factor of almost 2.5. For 95% burial, the amplitude of the backscattred time series has decreased significantly.

3.2 Solid aluminum cylinder

We now repeat many of the previous computations for a solid aluminum cylinder with the acousto-elastic parameters: $c_p = 6380$ m/s, $c_s = 3100$ m/s and $\rho = 2.79$ g/cm^3. In Figs. 6a-c we present the backscattered spectra for the same 15 levels of fractional burial as Figures 2. In Fig.6a the interference effects between the direct

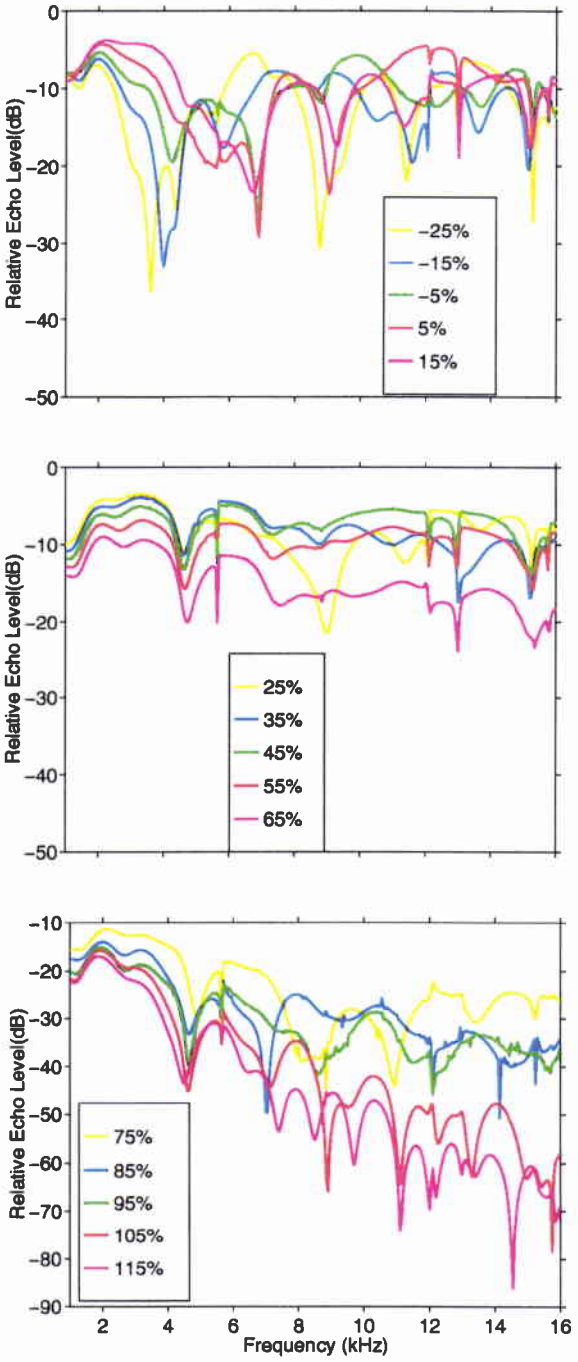

Figure 6: *Plots of backscattered power spectra from solid aluminum cylinder as a function of fractional burial, from above the seabed interface to totally buried.*

and seabed-reflected paths are evident. These effects disappear in Fig. 6b as the object becomes partially buried and the 5 curves seem qualitatively similar to one another. As the cylinder is increasingly buried in Fig. 6c, the level of backscatter decreases significantly and there is now additional interference effects in the spectra, but at a low amplitude level. The position of the null in the spectra at about 4.5 kHz changes slightly as a function of burial.

As in the previous example, we now compute the amplitude of the backscattered field for 5, 10, and 15 kHz as the cylinder's location varies from 1.5a above the seabed interface to 1.5a below. Although some of the details are different than for the steel shell case, the general features in Fig. 7 are the same as those of Fig. 3; there is some variation in the backscattered amplitude wth respect to the burial depth for the cylinder buried less than 50% and a rapid decrease in amplitude, especially for the 10 and 15 kHz curves after 50% burial. Finally we compute

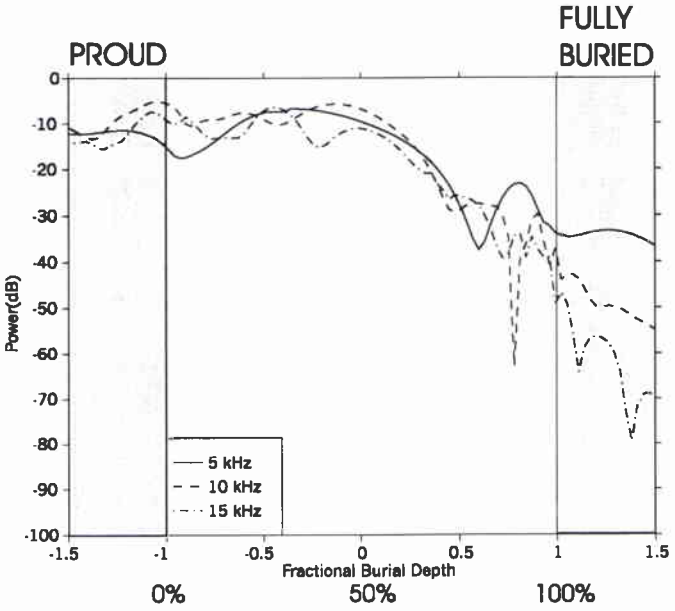

Figure 7: *Backscattered power levels from solid aluminum cylinder as a function of fractional burial for 5, 10, and 15 kHz.*

the backscattered time series for the different amounts of burial (Fig. 8). For this cylinder the specular reflection of the pulse has positive polarity because the solid cylinder "appears" rigid to the incident pulse (in contrast to the shell case where the interior was a pressure release surface). Above or partially above the seabed, the results of reflections from the seabed can be seen in the time series. These features disappear as the cylinder becomes approximately 50% buried. For 95% burial the backscattered series is diminished in amplitude and the arrival at approximately 2 ms, which appeared weakly in the 45% curve and in the free-space curve, is now almost equal in amplitude to the specular reflection.

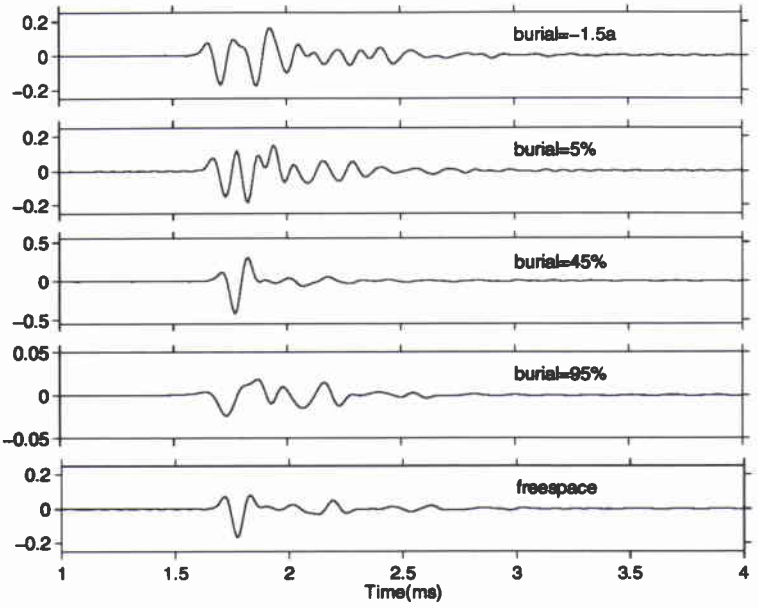

Figure 8: *Backscattered time series from solid aluminum cylinder as a function of fractional burial. (Please not the scale change and plots 3 and 4.)*

4

Summary

We have presented a method for computing exactly the scattering from a partially buried elastic cylinder. The form of the solution within the cylinder is utilized to specify the relation between the coefficients for the internal radial stress and the radial displacement. This relation is then used in the external BIEM to obtain a system of equations for the Fourier coefficients of the pressure field on the cylinder surface. There are some situations where the method may have difficulties due to the poor convergence properties of the series expansions, but, in general, the method performed well.

The backscattered spectra for a shelled and a solid cylinder as well as backscattered time series were computed for various amounts of burial. The incident field was a generalized plane wave (i.e., direct,reflected and transmitted components) with a subcritical grazing angle. For the cylinder above the seabed or only slightly buried, the spectra and the time series were complicated by the interferences between direct and seabed reflected paths. As the cylinder became close to 50% buried, the spectra and time series became simpler in structure and the amplitudes were larger than for the corresponding free-space result. After approximately 50% burial, the levels began to decrease rapidly with greater loss for higher frequencies. This is expected from the evanescent behaviour of the incident field in the bottom. The time series became smaller in amplitude for burial amounts greater than 50% with the higher frequency components of the incident spectrum being stripped out.

References

[1] J.A. Fawcett, "Modelling scattering from partially buried cylinders (Acoustic scattering from cylindrical objects embedded between two half-spaces/ The computation of the scattered pressure field from a cylinder embedded between two half-spaces with different densities)", SACLANTCEN SM-320, 1996.

[2] R. Lim, J.L. Lopes, R.H. Hackman, and D.G. Todoroff, "Scattering by objects buried in underwater sediments: Theory and experiment", J. Acoust. Soc. Am., **93**, pp. 1762–1783, 1993.

[3] R. Lim, "Acoustic scattering by a partially buried three-dimensional elastic object", J. Acoust. Soc. Am., **99**, p. 2498, 1996.

[4] D.T. DiPerna and T.K. Stanton, "Fresnel zone effects in the scattering of sound by cylinders of various lengths," J. Acoust. Soc. Am., **90**, pp.3348-3355, 1991.

[5] D.M.F. Chapman and F.D. Cotaras, "Acoustic backscattering from cylinders: near-field corrections," Canadian Acoustics, **19**, pp.71-72, 1991.

[6] I.B. Andreeva and V.G. Samovol'kin, "Sound scattering by elastic cylinders of finite length," Soviet Physics Acoustics, **22**, pp.363-364, 1976.

Document Data Sheet

Report no. changed (Mar 2006)

Security Classification		Project No.
		033-3
Document Serial No.	**Date of Issue**	**Total Pages**
SM-348	February 1998	20 pp.

Author(s)

Fawcett, J.A.

Title

Modelling of scattering by partially buried elastic cylinders

Abstract

The work of a previous memorandum on the modelling of scattering by a partially buried cylinder is extended to allow the cylinder to have full elasticity (and not just be a fluid structure as in the previous work). The results of computations showing the effects of increasing burial on the backscattered field, both in the spectral and temporal domains, are given. A shelled and a solid aluminium cylinder are considered for a grazing angle of incidence which is subcritical.

Keywords

cylinder – partially buried

Issuing Organization

North Atlantic Treaty Organization
SACLANT Undersea Research Centre
Viale San Bartolomeo 400, 19138 La Spezia, Italy

[From N. America: SACLANTCEN (New York) APO AE 09613]

Tel: +39 (0)187 527 361
Fax:+39 (0)187 524 600

E-mail: library@saclantc.nato.int

Report no. changed (Mar 2006): SM-348-UU

Initial Distribution for SM 348

Scientific Committee of National Representatives

SCNR Belgium	1	***National Liaison Officers***	
SCNR Canada	1		
SCNR Denmark	1	NLO Canada	1
SCNR Germany	1	NLO Denmark	1
SCNR Greece	1	NLO Germany	1
SCNR Italy	1	NLO Italy	1
SCNR Netherlands	1	NLO Netherlands	1
SCNR Norway	1	NLO Spain	1
SCNR Portugal	1	NLO UK	3
SCNR Spain	1	NLO USA	4
SCNR Turkey	1		
SCNR UK	1	Sub-total	30
SCNR USA	2	SACLANTCEN library	21
French Delegate	1		
SECGEN Rép. SCNR	1		
NAMILCOM Rep. SCNR	1	**Total**	51